Optical Engineering

OpticalEngineering.SPIEDigitalLibrary.org

Strain monitoring of bismaleimide composites using embedded microcavity sensor

Amardeep Kaur
Sudharshan Anandan
Lei Yuan
Steve E. Watkins
K. Chandrashekhara
Hai Xiao
Nam Phan

SPIE.

Strain monitoring of bismaleimide composites using embedded microcavity sensor

Amardeep Kaur,[a,*] Sudharshan Anandan,[b] Lei Yuan,[c] Steve E. Watkins,[a] K. Chandrashekhara,[b] Hai Xiao,[c] and Nam Phan[d]
[a]Missouri University of Science and Technology, Applied Optics Laboratory, 301 West 16th Street, Rolla, Missouri 65409-0040, United States
[b]Missouri University of Science and Technology, Composites Research Laboratory, 231 Toomey Hall, Rolla, Missouri 65409, United States
[c]Clemson University, Photonics Technology Laboratory, 209 Riggs Hall, 205 AMRL, Clemson, South Carolina 29634-0915, United States
[d]Naval Air Systems Command, Patuxent River, Maryland 20670-1906, United States

Abstract. A type of extrinsic Fabry–Perot interferometer (EFPI) fiber optic sensor, i.e., the microcavity strain sensor, is demonstrated for embedded, high-temperature applications. The sensor is fabricated using a femtosecond (fs) laser. The fs-laser-based fabrication makes the sensor thermally stable to sustain operating temperatures as high as 800°C. The sensor has low sensitivity toward the temperature as compared to its response toward the applied strain. The performance of the EFPI sensor is tested in an embedded application. The host material is carbon fiber/bismaleimide (BMI) composite laminate that offer thermally stable characteristics at high ambient temperatures. The sensor exhibits highly linear response toward the temperature and strain. Analytical work done with embedded optical-fiber sensors using the out-of-autoclave BMI laminate was limited until now. The work presented in this paper offers an insight into the strain and temperature interactions of the embedded sensors with the BMI composites. [DOI: 10.1117/1.OE.55.3.037102]

Keywords: optical-fiber sensor; extrinsic Fabry–Perot interferometer; bismaleimide; strain analysis; embedded sensors; structural monitoring.

Paper 151483P received Oct. 23, 2015; accepted for publication Feb. 12, 2016; published online Mar. 8, 2016.

1 Introduction

Repair and maintenance of structures demand a considerable amount of resources to be used each year. Embedded sensors as a component of smart structures technology can provide structural health information. Embedded sensors can give quality assurance in new structures or an estimate of remaining utility in aging structures. This capability provides an opportunity for preventive measures, e.g., performing repairs in time to prevent any major damage. Embedded fiber optic sensors have been used for cure monitoring, fatigue detection, strain profiling, and temperature measurement in the fields of aerospace, energy, and infrastructure.[1–4] Optical-fiber-based sensors have gained wide interest for structural health monitoring applications due to their compact size, immunity from electromagnetic interference, multiplexing capabilities, and so on. Different types of optical-fiber sensors such as fiber Bragg gratings,[1] extrinsic Fabry–Perot interferometric (EFPI) sensors,[2] intrinsic Fabry–Perot interferometric (IFPI) sensors,[5] long-period fiber gratings,[6] and combinations of these sensors[1] have been used in the field of structural health monitoring. High-temperature and embedded applications, however, impose significant limitations on the types of sensors that may be used. Optical-fiber sensors may be embedded in composite materials and structures with little material degradation. The embedded sensors must survive both the curing process and the environmental operating conditions.

In the work presented in this paper, high-performance carbon/bismaleimide (BMI) composite laminates are used. BMI-based composites are candidates for aerospace applications due to their superior strength and mechanical performance at elevated temperatures.[7] They are also easier to process as compared to other high-temperature materials such as polyimides. The composite laminates are manufactured using an out-of-autoclave (OOA) process. OOA processing has been shown to be capable of fabricating high quality epoxy laminates, but OOA processing of BMI is relatively new.[8,9] Previous work had established that laboratory scale OOA cured BMI composites can have properties similar to that of autoclave cured composites.[10] OOA BMI composites were also evaluated as part of a NASA Composites for Exploration program.[11,12]

Composites in aerospace applications can be exposed to harsh service conditions for high strain and fluctuating temperature. Optical-fiber sensors have gained wide interest for in-situ monitoring of the composite laminates and the most common parameter to be monitored for evaluating the in-service condition of the composite laminates is strain.[1,2] Among various optical-fiber-based sensors, EFPI-based sensors are best suited for strain monitoring applications under high ambient temperatures. Bragg gratings and IFPI sensors have been demonstrated for strain applications over the years,[5,13] but are very sensitive toward the ambient temperature as well. EFPI-based optical-fiber sensors have a low sensitivity toward the ambient temperature when compared to their sensitivity toward the strain. In addition to strain monitoring, EFPI sensors have been used to estimate the size of damage under impact loading.[14] Composite components used in airframes are also susceptible to barely visible impact damage (BVID), which are not easy to locate. Data from an array of fiber optic sensors can be used to locate the site of BVID, which can be of great importance in maintenance of composite structures.[15] However, many types of EFPI

*Address all correspondence to: Amardeep Kaur, E-mail: kaura@mst.edu

sensors cannot be used at high temperatures due to limitations of bonding epoxy. They are also difficult to calibrate. A microcavity EFPI strain sensor, fabricated using femtosecond (fs)-laser micromachining, avoids these limitations.[16] Cavity formation with fs-laser process yields stable structures that can withstand higher temperatures. Precise cavity dimensions can be used as compared to the traditional EFPI optical-fiber sensors or chemically etched, microcavity EFPI structures. Microcavity EFPI sensors with fs-laser fabrication have been shown to reliably operate up to 800°C.[16]

The microcavity EFPI strain sensor is applied for embedded, high-temperature operation to investigate a new composite material and test the sensor's embeddability. The sensor has a very low sensitivity toward the ambient temperature as compared to its strain sensitivity thus making it an ideal choice for strain monitoring at high temperatures. The sensor performance is shown for an embedded application in BMI composite laminates. The microcavity sensor survived the curing process at 190.56°C and provided reliable strain measurements at operating temperatures up to 225°C. The glass transition temperature of the BMI resin limited the highest tested temperature limit for the embedded sensor. Measurement performance, strain transfer, and thermal behavior are discussed. Analytical work done using the OOA BMI laminates was limited in nature until now. The work presented in this paper offers a new insight into the strain and temperature interactions of the embedded sensors with the BMI and demonstrates the embeddability of the microcavity EFPI sensor in composite materials.

2 Microcavity Extrinsic Fabry–Perot Interferometer Sensor Design and Instrumentation

The EFPI sensor consists of two reflective surfaces created by fabricating a cavity. Figures 1(a) and 1(b) show a traditional cavity-based EFPI sensor design and the microcavity EFPI design, respectively. Input light traveling in the core of the fiber reflects from the two walls of the cavity and the difference (induced by the cavity length change) between these two reflections, in turn, causes a wavelength shift in the original input signal. This wavelength shift is a measure of change in the cavity length. In a strain sensor with an air gap of length d, the gauge length is approximately the tube length L, and the measured strain is $\Delta L/L = \Delta d/d$.

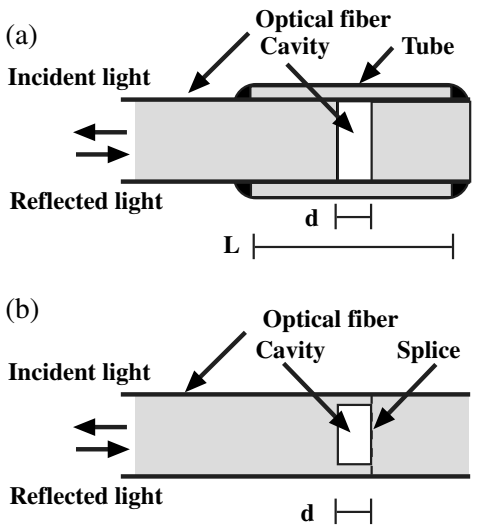

Fig. 1 Sensors: (a) traditional tube-based EFPI and (b) microcavity EFPI.

Traditionally, the cavity in an optical-fiber sensor is formed using two pieces of optical fiber, aligned and bonded to a capillary tube using an epoxy adhesive.[17,18] The use of epoxy introduces a temperature limitation, e.g., the maximum temperature for Loctite epoxy is 225°C once cured. Moreover, the tube component causes the design to be bulkier and difficult to fabricate. The exact gauge length and the initial gap length are difficult to determine for the traditional design; hence, calibration is an issue.

The microcavity sensor has a low sensitivity to the thermal environment. Thermal expansion of the EFPI depends upon the thermo-optic coefficient and the coefficient of thermal expansion (CTE). Thermo-optic coefficient further depends upon the refractive index of the medium of the cavity (air). Thus, the low CTE of silica (0.55×10^{-6}/°C) makes the single-mode silica fiber an ideal candidate to be used for high-temperature applications.[16]

3 Manufacturing

3.1 *Microcavity Extrinsic Fabry–Perot Interferometer Sensor Fabrication*

The cavity is fabricated by etching a 35-μm-deep square surface (65 μm × 65 μm) on the tip of a single-mode fiber using a laboratory-integrated fs-laser micromachining system [Fig. 1(b)]. The sensor fabrication is completed by fusion splicing another single-mode fiber to the ablated cavity.[16] This process allows the use of small gauge lengths with increased sensitivity. The exact gauge length and gap can be determined easily, reducing calibration issues and repeatability issues. The gap in the microcavity sensor benefits by having an exposed cavity that is created from a well-characterized laser etching process.[16] By contrast, the gap in the tube-based sensor is not exposed and is formed from a mechanical positioning and epoxying process.

3.2 *Bismaleimide Composite Sample Fabrication*

The host material for the embedded testing was carbon fiber/BMI composite (laminates). For results presented here, six-layer unidirectional laminates were fabricated (12 in. × 1 in.) using IM7G/AR4550 prepreg by OOA process. The ply orientations of the six layers were $[0\ \text{deg}/90\ \text{deg}/0\ \text{deg}]_s$. A microcavity EFPI sensor was placed between the central layers. Figure 2 shows the arrangement of the BMI laminate layers and the sensor placement. The approximate location of the sensor was at [6 in., 0.5 in.]. A heat shrinking tube was used at the egress point to prevent damage to the optical fiber due to high stress concentrations. The prepreg layup was cured at 190.56°C for 2 h. The samples were then postcured at 200°C.

4 Experimentation

Mechanical and thermal tests were conducted on free sensor as well as sensor embedded in BMI composites. In case of embedded sensor, strain transfer was evaluated after green body cure at a curing temperature of 190.5°C and after a free-standing postcure at 200°C. Term green body[19] is used for the fiber-reinforced polymers or ceramics that are held in shape

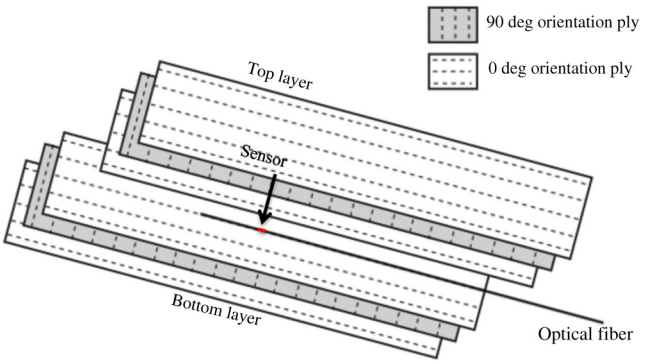

Fig. 2 Embedded sample layout with the sensor embedded in the middle.

Table 1 Testing parameters for embedded and free sensors.

Sensor	Testing parameter	Lower limit tested	Upper limit tested	Response factor
Free	Temperature	50°C	800°C	Wavelength shift
Embedded	Temperature	50°C	225°C	Wavelength shift
Free	Strain	0 $\mu\varepsilon$	3700 $\mu\varepsilon$	Wavelength shift
Embedded	Strain	0 $\mu\varepsilon$	4000 $\mu\varepsilon$	Wavelength shift

by mechanical pressing. Details of testing parameters are shown in Table 1.

Figure 3 shows the instrumentation used for the EFPI sensor testing. A 100-nm (1520 to 1620 nm) broadband source (B&W Tek Inc.) with a resolution of 0.01 nm was used as input, a 3-dB coupler was used to send the signal to the sensor and receive the reflected signal back. This signal was then recorded using an optical spectrum analyzer (OSA). The wavelength shift in the return spectra is linearly dependent upon the strain, $\Delta d/d$ where d is the cavity length and Δd is the change in the cavity length resulted either from thermal expansion or applied strain.[16] With the application of axial strain, the cavity length d will change inducing a change in the central wavelength, λ, resulting in a wavelength shift, $\Delta\lambda$. For a precise measurement, a sharp valley (or dip) was tracked for the wavelength shift. The OSA used was capable of storing the reflected spectra at regular intervals. A MATLAB code was then used for signal processing (in CSV format) and determining the wavelength shift for strain as well as temperature applications.

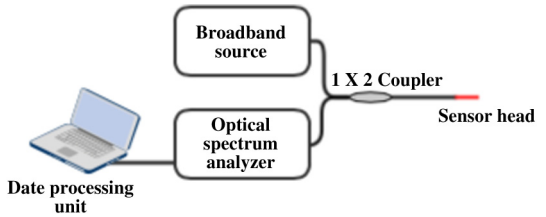

Fig. 3 The instrumentation setup for sensor testing and response monitoring.

Table 2 Properties of the BMI composite.

Parameter	Value
Sample size used for embedding the sensor	12 in. × 1 in. (304.8 mm × 25.4 mm)
Glass transition temperature	271°C
Cure temperature	190.55°C
Tensile modulus	142 GPa
Major Poisson ratio (ν_{12})	0.29

4.1 *Temperature Response*

To test the temperature response of the free sensor, the optical fiber was placed inside a box furnace (Lindberg/Blue M) and heated from room temperature to 800°C in steps of 50°C. The resultant wavelength shift in the spectrum was recorded.

The temperature response of the embedded sensor was evaluated in a similar manner. A sample with the embedded sensor was placed in the box furnace and heated to 225°C in steps of 25°C. The glass transition temperature (271°C) of the BMI resin limited the upper limit of the temperature tested. Table 2 lists some of the properties of the BMI resin used in the carbon-reinforced fiber laminates used for embedded sensor testing. Figure 4 shows the microscopic image of the embedded sensor in a tested sample. Note the quality of the interface between the BMI structure and the optical-fiber sensor.

4.2 *Strain Response*

For the strain testing of the free sensor at room temperature, the sensor was fixed to translation stages (Newport) at both the ends. A certain amount of prestrain was applied in order to remove slack in the optical fiber. An axial strain was induced along the optical fiber/sensor axis resulting in a wavelength shift in the reflection spectra.

Tensile tests on embedded sensor samples were conducted on an Instron 5985 universal testing machine. A strain controlled test was performed, and the wavelength shift was recorded every 500 $\mu\varepsilon$. Figure 5 shows a composite sample with embedded sensor between the grips of the test equipment. A longitudinal split, i.e., sample failure can also be seen; optical-fiber sensor also failed when the BMI laminate

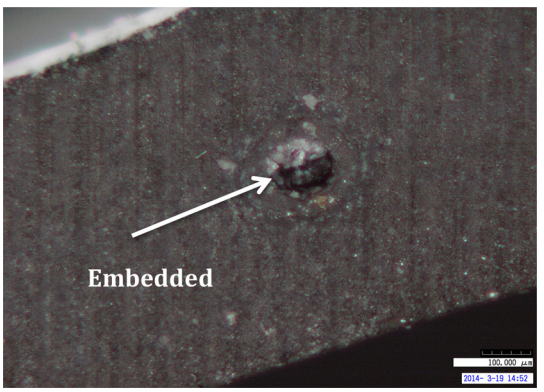

Fig. 4 Microscopic image of the embedded sensor.

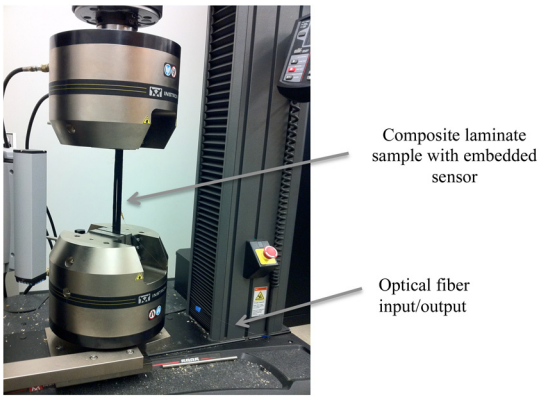

Fig. 5 INSTRON machine used for strain testing of the embedded sensor.

sample failed. For testing the sensor's strain performance at elevated temperatures, an environmental test chamber was used.

5 Results and Discussions

In this section, the experimental results for temperature and strain responses of the sensor are presented and discussed. Results for testing in free and embedded environments are presented. Similar EFPI sensors were used to produce the results presented; fringe visibility of the sensors ranged from 12 to 20 dB and the cavity length was 35 μm.

5.1 *Temperature Response*

Figure 6 shows the wavelength shift and the thermal strain resulting from the increasing ambient temperature as observed by using the free and embedded EFPI sensor.

For the free sensor, the slope of the response was calculated to be 0.6 pm/°C and CTE of the silica was calculated to be 0.715×10^{-6}/°C which is 1.3 times larger than that of the actual CTE. The slope and CTE calculated from the sensor embedded in BMI composites were calculated to be 1.7 pm/°C and 1.615×10^{-6}/°C, respectively. The composite CTE can be calculated to be 0.028×10^{-6}/°C using[20]

Table 3 Properties used in Eq. (1).

Parameter	Value
Fiber elasticity, $\mathbf{E_f}$	4830 MPa (material datasheet)
Matrix elasticity, $\mathbf{E_m}$	48.26 MPa (transverse tensile strength of composite, material datasheet)
Fiber volume fraction, $\mathbf{V_f}$	0.5766
Matrix volume fraction, $\mathbf{V_m}$	0.4344
Composite fiber CTE, $\boldsymbol{\alpha_f}$	-0.6×10^{-6}/°C (material datasheet)
Matrix CTE, $\boldsymbol{\alpha_m}$	44×10^{-6}/°C[21]

$$\alpha_c = \frac{E_f V_f \alpha_f + E_m V_m \alpha_m}{E_f V_f + E_m V_m}. \quad (1)$$

The terms in Eq. (1) are shown in Table 3.

The composite CTE calculated using the embedded optical fiber was higher than the CTE calculated using Eq. (1), and about 2.3 times larger than the calculated CTE of silica. For the free sensor, the thermal strain resulting from the cavity expansion was 0.37 $\mu\varepsilon$/°C whereas the strain exerted on the embedded sensor was calculated to be 1.11 $\mu\varepsilon$/°C. Larger strain in the case of the embedded sensor is due to the effect of the interfacial bond between optical fiber and the surrounding composite material. The sensor is not very sensitive toward the temperature, but it does respond very well toward the thermal strain of the host structure. For both the embedded and free sensors, the correlation coefficient was 0.99, demonstrating a highly linear response.

5.2 *Strain Response*

Strain response of the free and the embedded sensors at room temperature is presented in Fig. 7. The response for both the sensors toward strain is highly linear with a correlation coefficient of 0.99. The free sensor had a strain transfer of 0.98 $\mu\varepsilon/\mu\varepsilon$ indicating a good agreement between measured

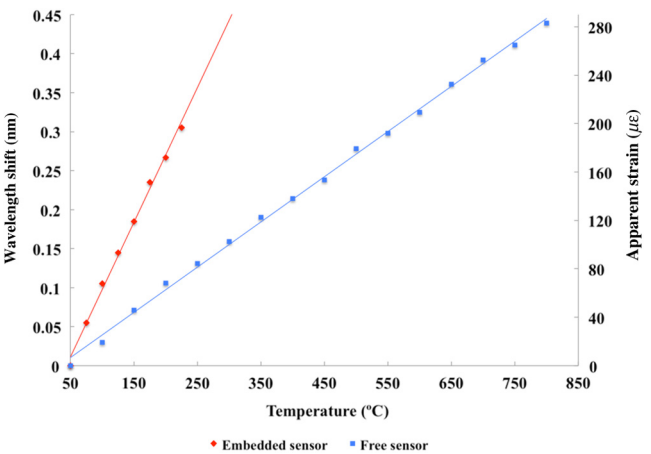

Fig. 6 Response of the embedded (in carbon fiber-reinforced composites) and free EFPI sensors toward the ambient temperature.

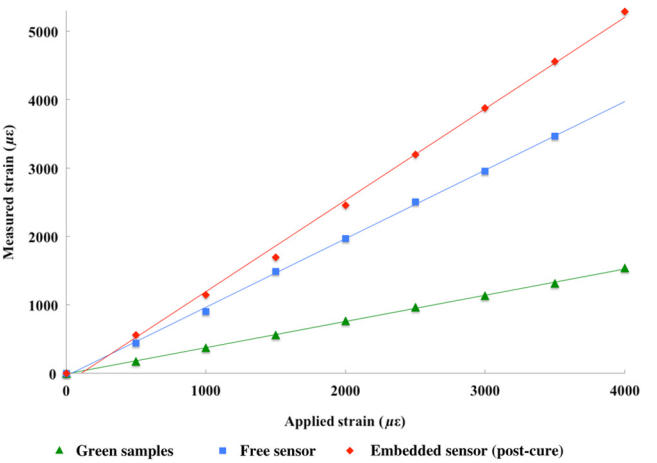

Fig. 7 Measured strain response of the embedded and the free sensors at room temperature.

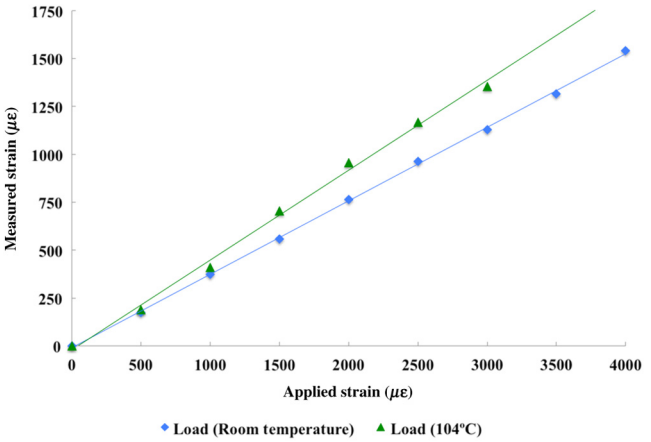

Fig. 8 Measured strain response of the embedded sensor at room temperature and at 104.4°C.

strain and applied strain. For the free sensor, the strain was applied until the fusion joint broke loose from the cavity; it was verified under a microscope that the cavity broke at the fusion joint. The breaking point for the EFPI was observed to be at 3800 $\mu\varepsilon$.

The strain response of the embedded sensor was evaluated after green body cure and a postcure cycle. The strain transfer for the embedded sensor after green body was 38 $\mu\varepsilon/\mu\varepsilon$, while the strain transfer of the embedded sensor after postcuring was 1.28 $\mu\varepsilon/\mu\varepsilon$. The embedded sensors in green samples underpredict the strain, while the sensors in postcured samples overpredict the applied strain levels. Postcuring results in a change in degree of cure and crosslinking in thermosetting resins. Residual stresses are also developed due to cure shrinkage and the difference in CTE between the carbon fibers and matrix. These can result in a difference in strain response between a green body and a postcured sample.

The sensor was also used to observe the strain response in an embedded environment at an elevated temperature of 104.4°C. The results are presented in Fig. 8. The ambient temperature of 104.4°C yielded a response with a slightly higher slope. Because of the low sensitivity of the sensor toward the temperature, the difference in the slopes was 1 pm/$\mu\varepsilon$. For electrical strain gauges and strain applicator, strain on the order of 100 $\mu\varepsilon$ is considered as noise. As demonstrated in the Fig. 8, apparent strain added by a temperature raise of 104.4°C is less than 200 $\mu\varepsilon$, which is acceptable for most regularly monitored civil and aerospace infrastructures. Due to low temperature sensitivity of the microcavity sensor, cross-sensitivity does not pose a high risk for previously mentioned applications. If the temperature variations and strain variations are larger, cross-sensitivity and material dependent strain transfer should be considered.

6 Conclusions

A microcavity EFPI fiber optic sensor for the measurement of strain in BMI composites is presented in this paper. The silica material of the optical-fiber sensor and the thermal stability resulting from the fs-laser fabrication enable the sensor to have excellent properties for embedded applications and for high-temperature applications. Although the sensor itself has been shown to handle temperatures up to 800°C, it was limited in this work to the glass transition temperature (271°C) of the BMI composite. A single fusion joint allows for better structural integrity and ease-of-fabrication over tube-encapsulated designs. The inherent properties of the fused silica and the EFPI cavity structure enable the sensor to be used as an efficient strain sensor. The responses of a free sensor as well as a sensor embedded in OOA cured carbon/BMI composite laminates were evaluated. The microcavity EFPI sensor survived the composite cure process.

Temperature and strain responses are demonstrated for the free and the embedded sensors. The sensors provided reliable thermal strain measurements at operating temperatures up to 225°C. The sensors demonstrated a highly linear response toward temperature and strain; the coefficient of linearity was 0.98 or higher for both responses. The temperature sensitivity of the free and embedded sensors was 0.6 and 1.7 pm/°C, respectively. The resulting cavity expansion exerted a thermal strain amounting to 0.37 $\mu\varepsilon$/°C for the free sensor and 1.11 $\mu\varepsilon$/°C for the embedded sensor. There were expected differences in the slopes of the responses and the CTE values calculated for silica were higher than the actual CTE of the silica. However, the sensor responds linearly toward the temperature increase and the wavelength shift is small at temperatures as high as 800°C as compared to its strain sensitivity. The fitting linearity for both the temperature and strain response was 0.99.

Strain response of the free and the embedded sensors was also evaluated. The strain sensitivity of the free sensor was 1.5 and 0.6 pm/$\mu\varepsilon$ for the embedded sensor for green samples. Incorporating a freestanding postcure during manufacturing of embedded samples resulted in an increase in strain transfer from 0.38 to 1.28 $\mu\varepsilon/\mu\varepsilon$. This improvement can be a result of increased degree of cure and a change in residual stresses in the composite. Ongoing work is examining the repeatability of the embedded sensor performance. Due to some little material properties (of BMI composites), more work needs to be done in order to explain conclusively the residual strain behavior in the data obtained from repeatability tests.

An ease-of-fabrication, small size, embedding capability, low temperature, and high strain sensitivity for carbon fiber composite laminates makes this sensor a very good candidate for strain monitoring applications in high ambient temperatures. The work also provides new insight into the behavior of BMI composite laminates, especially the strain transfer interaction between the sensors and the laminates. The strain endured by commonly monitored structures such as airframes, bridges, and so on, is above 500 $\mu\varepsilon$ and the temperature variation for regular operations is not more than a few tens of degrees Celsius. Due to low temperature sensitivity of the microcavity sensor, cross-sensitivity does not pose a high risk for previously mentioned applications. If the temperature variations and strain variations are larger, cross-sensitivity and material-dependent strain transfer should be considered.

Acknowledgments

The authors acknowledge the support of National Science Foundation project under Grant CMMI-1200787. This research was sponsored in part by Integrated Systems Solutions, Inc. The authors would like to thank Stratton Composite Solutions for the materials supplied.

References

1. V. M. Murukeshan et al., "Cure monitoring of smart composites using fiber Bragg grating based embedded sensors," *Sens. Actuators A* **79**, 153–161 (2000).
2. J. Etches and G. Fernando, "Evaluation of embedded optical fiber sensors in composites: EFPI sensor response to fatigue loading," *Polym. Compos.* **31**, 284–291 (2010).
3. V. Zetterlind, S. Watkins, and M. Spoltman, "Fatigue testing of a composite propeller blade using fiber optic strain sensor," *IEEE Sens. J.* **3**(4), 393–399 (2003).
4. V. Bhatia et al., "Optical fiber extrinsic Fabry–Perot interferometric strain sensor for multiple strain state measurements," *Proc. SPIE* **2444**, 115–126 (1995).
5. Z. Huang et al., "Intrinsic Fabry–Perot fiber sensor for temperature and strain measurements," *IEEE Photonics Technol. Lett.* **17**(11), 2403–2405 (2005).
6. S. Zheng, "Long-period fiber grating moisture sensor with nano-structured coatings for structural health monitoring," *Struct. Health Monit.* **14**(2), 148–157 (2015).
7. M. Stenzenberger et al., "Bismaleimide resins: past, present, future," in *Proc. of the Int. SAMPE Symp. and Exhibition*, Reno, NV, pp. 1877–1888 (1989).
8. T. Centea, L. Gunenfelder, and S. Nutt, "A review of out-of-autoclave prepregs—material properties, process phenomena, and manufacturing considerations," *Composites Part A* **70**, 132–154 (2015).
9. R. Stratton and L. Repecka, "Demonstration of next generation BMI prepregs for out-of-autoclave processing," in *Proc. of the Int. SAMPE Technical Conf.*, Long Beach, CA, pp. 1–10 (2011).
10. S. Anandan et al., "Post-curing effects on out-of-autoclave BMI panels," in *Proc. of the Int. SAMPE Technical Conf.*, Seattle, WA, pp. 1–11 (2014).
11. W. Hastings et al., "Fabrication and characterization of out-of-autoclave (OOA) bismaleimide (BMI) laminates for large composite structures," in *Proc. of the Int. SAMPE Technical Conf.*, Long Beach, CA, pp. 1347–1360 (2013).
12. T. Hou et al., "Out-of-autoclave processing and properties of bismaleimide composites," *J. Reinf. Plast. Compos.* **33**, 137–149 (2014).
13. M. Majumder et al., "Fiber Bragg gratings in structural health monitoring—present status and applications," *Sens. Actuators A* **147**(1), 150–164 (2008).
14. G. P. Carman et al., "Micro-damage analysis with embedded sensors in macro-composites," in *Proc. of Active Materials and Adaptive Structures Session ADPA/AIAA/ASME/SPIE*, pp. 567–572 (1997).
15. G. Zhou and L. M. Sim, "Damage detection and assessment in fibre-reinforced composite structures with embedded fibre optic sensors-review," *Smart Mater. Struct.* **11**, 925–939 (2002).
16. A. Kaur et al., "Micro-cavity based strain sensor for high temperature applications," *Opt. Eng.* **53**(1), 017105 (2014).
17. A. D. Kersey, D. A. Jackson, and M. Corke, "A simple fiber Fabry–Perot sensor," *Opt. Commun.* **45**, 71–74 (1983).
18. T. Gangopadhyay, "Prospects for fibre Bragg gratings and Fabry–Perot interferometers in fibre-optic vibration sensing," *Sens. Actuators A* **113**, 20–38 (2004).
19. M. Balasubramanian, *Composite Materials and Processing*, CRC Press, Florida (2014).
20. Z. Ran et al., "Determination of thermal expansion coefficients for unidirectional fiber reinforced composites," *Chin. J. Aeronaut.* **27**(5), 1180–1187 (2014).
21. J. Nelson et al., "Development of nano-silica bismaleimide (BMI) matrix resins for prepeg tooling composites: fortified tooling prepeg BMI," in *SAMPE Technical Conf.*, May 21–24, Baltimore, MD, pp. 1–13 (2013).

Amardeep Kaur is an assistant teaching professor in electrical and computer engineering at the Missouri University of Science and Technology (Missouri S&T). She received her PhD from Missouri S&T. Her research interests include micro/nanofabrication of optical-fiber sensors, structural health monitoring, embedded sensing, and engineering education. She is a member of SPIE, IEEE, ASEE, SWE, and IEEE-HKN honor society.

Sudharshan Anandan is pursuing his PhD in mechanical engineering at the Missouri University of Science and Technology (Missouri S&T). He received his BTech in mechanical engineering from National Institute of Technology, Karnataka, India, in 2009, and his MS degree in mechanical engineering from Missouri S&T in 2013. His research focuses on manufacturing, testing, and numerical modeling of composite materials.

Lei Yuan received his BS degree in mechanical engineering from Beijing University of Aeronautics and Astronautics, Beijing, China, in 2008. He is currently pursuing his PhD in electrical engineering at Clemson University, Clemson, SC, USA. His research interests mainly focus on laser micro/nanofabrication as well as fiber optical sensors and devices for various engineering applications. He is a student member of OSA and SPIE.

Steve E. Watkins is a professor of electrical and computer engineering and director of the Applied Optics Laboratory at the Missouri University of Science and Technology (formerly the University of Missouri-Rolla). He received a PhD from the University of Texas at Austin in 1989. His memberships include SPIE (senior member), IEEE (senior member), and ASEE. He was an IEEE-USA Congressional Fellow, a visiting physicist at the Phillips Laboratory (USAF), and a visiting scholar at the NTT in Japan.

K. Chandrashekhara is a curators' professor of mechanical and aerospace engineering at the Missouri University of Science and Technology, Rolla, MO, USA. His expertise is in the area of composite materials and finite element analysis. He has published over 250 refereed papers, including over 100 journal articles and has been granted one U.S. patent.

Hai Xiao is the Samuel Lewis Bell distinguished professor of electrical and computer engineering at Clemson University. He received his PhD in electrical engineering from Virginia Tech. Previously he was a professor of electrical engineering and director of the Photonics Technology Laboratory at the Missouri S&T. He is the recipient of prestigious awards, including the Office of Naval Research Young Investigator Program Award (2006), the R&D 100 Award (2004), and the Virginia Tech Outstanding Achievement Award (2003).

Nam Phan is an aerospace engineering supervisor in the Structures Division, NAVAIR Systems Command, Patuxent River, MD, USA. His expertise is on aircraft structures for sea-based aviation applications.